Materials Research Express

PAPER

Evaluation of thermal, mechanical, electrical and optical properties of metal-oxide dispersed HDPE nanocomposites

M T Rahman[1], Md Asadul Hoque[1], G T Rahman[1], M A Gafur[2], Ruhul A Khan[3] and M Khalid Hossain[3,4]

[1] Dept. of Materials Science & Engineering, University of Rajshahi, Rajshahi 6205, Bangladesh
[2] Pilot Plant and Process Development Center, Bangladesh Council of Scientific and Industrial Research, Dhaka 1205, Bangladesh
[3] Atomic Energy Research Establishment, Bangladesh Atomic Energy Commission, Dhaka, Bangladesh
[4] Dept. of Advanced Energy Engineering Science, IGSES, Kyushu University, Fukuoka 816-8580, Japan

E-mail: khalid.baec@gmail.com

RECEIVED
13 February 2019

REVISED
14 May 2019

ACCEPTED FOR PUBLICATION
20 May 2019

PUBLISHED
29 May 2019

Keywords: high density polyethylene, nanocomposites, tensile test, TGA analysis, electrical resistivity, optical bandgap

Abstract

In this work, synthesized Fe_2O_3, TiO_2 and $NiFe_2O_4$ nanoparticles dispersed high density polyethylene (HDPE) polymer matrix based Fe_2O_3/HDPE, TiO_2/HDPE, $NiFe_2O_4$/HDPE and (Fe_2O_3/TiO_2/$NiFe_2O_4$/HDPE) nanocomposites were fabricated. A comparative study on their thermal properties, mechanical properties, optical properties, and DC electrical properties were performed. The highest Young's modulus was found in the Fe_2O_3/HDPE composite which is 30.47% higher than the pure HDPE polymer alone. Hardness was improved in all composites, except for $NiFe_2O_4$/HDPE nanocomposite. Decreased resistivity was observed in $NiFe_2O_4$/HDPE composite only. The highest light absorption in UV–vis range was found in (Fe_2O_3/TiO_2/$NiFe_2O_4$)/HDPE composite, also, the lowest optical band gap energy was found in TiO_2/HDPE nanocomposite which is 48.88% lower than the pure HDPE polymer alone. All HDPE based nanocomposites showed improved thermal, mechanical, electrical and optical properties and they can be used in biomedical and electronic devices.

1. Introduction

Inorganic nanoparticles dispersed polymeric composites possess unique and excellent properties because of the synergic effect of nanoparticles and polymer matrix. With the improvement of mechanical properties of host polymer the nanoparticles also help to induce variable electrical, optical, mechanical and thermal properties [1]. This induced novel physio-chemical properties make them a popular candidate for several applications. The recent development of nanoscience and nanotechnology has enabled the production of various nanoparticles. Therefore, a variety of nanoparticles can be added to polymer matrices in order to produce polymer nanocomposites with desirable properties for increasing application.

High density polyethylene (HDPE) is one of the most demanding engineering plastics which expanding its application continuously due to its regular chain structure, flexibility, low cost, low processing energy, easy to process by most methods, excellent biocompatibility, good chemical resistance, weatherproof and good mechanical strength [2]. Generally pure HDPE has been used as plastic bottles, toys, chemical containers, pipe systems, ballistic plates, fuel tanks and plastic surgery. Also, HDPE based nanocomposites have been used in food packaging, barrier applications, dielectric material, conducting composite and biomedical applications [3, 4]. However, several properties of HDPE can be improved by the addition of nanoparticles into this polymer matrix and can be used as potential materials in both industrial and biomedical sectors [5].

Iron oxide i.e. hematite (α-Fe_2O_3) is the most stable form of iron and extensively used as filler material in nanocomposites for low cost, biocompatibility, corrosion resistance and non-toxicity properties [6]. Due to having different physical and chemical properties, iron oxide-based nanocomposites have been used as magnetic and microwave absorber, electrode for supercapacitor, EMI shielding, bioanalytical sensors, refrigeration and high-density information storage [7, 8].

Titanium dioxide (TiO_2) belongs to the family of transition metal oxides. It is inert, non-toxic and cheap in nanocomposite fabrication [9]. Nanocomposites based on TiO_2 nanoparticles are being used successfully in solar cells, coatings, electron transport layer, membrane distillation, and food processing sectors [10, 11]. Nickel ferrite ($NiFe_2O_4$) is one of the most important spinel ferrites that have been studied. It exhibits distinctive physical and chemical properties when its size is reduced to nano size. This ferrite is particularly attractive to researchers due to its high magnetocrystalline anisotropy, high saturation magnetization, unique magnetic structure [12] magnetic separability, chemical stability and photocatalytic property [13]. It exhibits distinctive physical and chemical properties when its size is reduced to nano size. At nano size nickel ferrite exhibits distinctive physical and chemical properties, therefore, composites based on these nanoparticles have been used extensively as electrodes for super capacitor, drug delivery, modifier for electrochemical sensor, cholesterol biosensor and microwave absorber [14, 15].

In previous studies, many researchers fabricated high density polyethylene based polymer composites such as Hydroxyapatite/HDPE [16], SiO_2/HDPE [17], MMT/HDPE [18], MWCNTs/HDPE [19], BN/HDPE [20], and clay/HDPE [21]. However, minor importance was given to investigate the synergic effect of Fe_2O_3, TiO_2 and $NiFe_2O_4$ nanoparticles in a polymeric system. Therefore, in view of mentioned advantages and vast utility above, it is necessary to investigate the individual and mutual effect of those nanoparticles in HDPE polymer composite.

The aim of this work is to fabricate high density polyethylene based nanocomposites using 5 wt% of synthesized Fe_2O_3, TiO_2, $NiFe_2O_4$ as well as (Fe_2O_3/TiO_2/$NiFe_2O_4$) nanoparticles as reinforcement. Also, perform a comparative study to evaluate the mechanical, thermal, electrical and optical properties of those fabricated composites. According to the applications and scopes discussed above, these newly fabricated nanocomposites could be potentially useful for biomedical as well as many industrial purposes.

2. Materials and methods

2.1. Materials

The chemicals and materials used in this research were: anhydrous ferric nitrate $Fe(NO_3)_3$ (Merck, India), anhydrous citric acid $C_6H_8O_7$ (Merck, India), titanium isopropoxide $Ti[OCH(CH_3)_2]_4$ (Sigma-Aldrich, Germany), iso-propyl alcohol $(CH_3)_2CHOH$ (Sigma-Aldrich, Germany), Anhydrous nickel chloride $NiCl_2$ (Merck, India), anhydrous ferric chloride $FeCl_3$ (Merck, India), sodium hydroxide NaOH (Merck, India), high density polyethylene (HDPE) (Nasim Chemicals Ltd, BD).

2.2. Synthesis of nanoparticles

Iron oxide nanoparticles were synthesized chemically following modified sol-gel method [22] by dropwise addition of 200 ml (0.1 M) iron nitrate ($Fe(NO_3)_3$) and 800 ml (0.1 M) citric acid ($C_6H_8O_7$) solution under vigorous stirring. This mixture was heated to 70 °C under continuous stirring until the gel formation and the gel was then dried by evaporation. The dried gel was annealed at 250 °C for 2 hours, cooled, and grinded by mortar and pestle to get Fe_2O_3 nanopowder.

Titanium dioxide nanoparticles were synthesized chemically following modified sol-gel [23] method by mixing 15 ml titanium isopropoxide ($Ti[OCH(CH_3)_2]_4$) and 100 ml iso-propyl alcohol ($(CH_3)_2CHOH$) and stirred 10 min vigorously. Further, dropwise 10 ml de-ionized water was added to the mixed solution for gel formation under continuous stirring for 2 hours. The gel was then left for 24 hours in a dark place for aging. After ageing it was dried in an oven and annealed at 550 °C for 2 hours to get white TiO_2 nanopowder.

Nickel ferrite nanoparticles were synthesized chemically following modified co-precipitation method [24] by mixing 100 ml (0.2 M) nickel chloride ($NiCl_2$) and 100 ml (0.4 M) ferric chloride ($FeCl_3$) solution. Later, 3 M solution of sodium hydroxide (NaOH) was added dropwise under vigorous string until a p^H level >12 was reached and the mixture solution was heated for 60 min at 80 °C with vigorous stirring. The produced black precipitate was filtered using filter paper. The product was then washed several times with distilled water and ethanol as well as dried overnight above 80 °C. Later, the dried product was annealed for 4 hours at 250 °C and grinded to get fine $NiFe_2O_4$ nanopowder.

2.3. Fabrication of nanocomposites

Synthesized Fe_2O_3, TiO_2, and $NiFe_2O_4$ nanoparticles based HDPE polymer matrix nanocomposites were fabricated by hot compression molding method (Carver-4128, Model 30–12 H, USA) at temperature 155 °C. To prepare a composite sheet, Fe_2O_3 nanopowder (5 wt%) and HDPE granules were placed between two brass plates. When the temperature of both upper and lower plates reached 155 °C, the sample was melted for 8 min and then 5 tons pressure was applied for 3 min. After proper cooling the pressure was released and the fabricated sample was taken out. As the HDPE polymer is in granular form and Fe_2O_3 is in powder form, therefore, for well dispersion of nanomaterials in polymer matrix the fabricated sheet was cut into very small pieces and repeated

the method as described above. Thus, the polymer nanocomposites of 1 mm thickness were fabricated, where the thickness was confirmed by using a digital caliper (Mitutoyo, Series: 500/300 mm, Japan).

TiO_2, $NiFe_2O_4$, and (Fe_2O_3/TiO_2/$NiFe_2O_4$) nanoparticles filled polymer nanocomposites were fabricated following the same method as described above, where TiO_2 (5 wt%), $NiFe_2O_4$ (5 wt%), and 1.66 wt% Fe_2O_3 + 1.66 wt% TiO_2 + 1.66 wt% $NiFe_2O_4$ nanoparticles were used as filler materials respectively instead of Fe_2O_3 nanoparticles.

2.4. Characterization

Synthesized nanoparticles were characterized by XRD, SEM and EDS analysis. XRD patterns of the synthesized nanoparticles were taken by an x-ray diffractometer (BRUKER D8 ADVANCE, GERMANY). The diffraction patterns were recorded at room temperature using Cu Kα radiation (λ = 1.5406 Å) for Bragg's angle varying from 10° to 70°, and particles size were measured using Debye-Scherer equation, where k = 0.94 and λ = 0.154 06 nm [25, 26]. The surface morphology of the nanoparticles was observed using FE-SEM (JEOL, JSM-7610F, JAPAN) operated at 10 kV. During the SEM test, EDS data was taken from the same sample.

Fabricated nanocomposites thermal, mechanical, micro-hardness, DC electrical, and optical properties were also characterized. The mechanical properties i.e. tensile strength, elastic modulus and fracture of the fabricated composites were measured by a universal Testing Machine (HOUNSFIELD, H10KS, UK) with a 2 mm min^{-1} speed and 25 mm gauge length. The hardness of the nanocomposites was investigated using micro hardness tester (SHIMADZU, HMV-2, JAPAN) at 98.07 mN, 245.2 mN, and 490.3 mN load range for 10 s indentation time with 5 times repetition for each sample. The DC analysis was done by an electrometer (KEITHLEY, 6517B, USA) varying voltage from 0 to 40 V to measure output current. The DC electrical measurement was done by following two probe method. The optical absorption was measured using UV–Vis spectrophotometer (SHIMADZU, UV-1601, JAPAN) in the range of 190–1100 nm and optical band gap energy was calculated using Tauc's plot [27].

3. Results and discussion

3.1. XRD analysis of nanoparticles

All XRD spectra for synthesized Fe_2O_3, TiO_2, and $NiFe_2O_4$ nanoparticles are illustrated in figure 1 and the obtained data is tabulated in table 1. According to the figure 1, the peaks appeared at the 2θ range can be indexed to crystalline hematite (α-Fe_2O_3), anatase (TiO_2), and inverse spinel structure of $NiFe_2O_4$ respectively by comparison with JCPDS Card File No. 33–0664, 21–1272, and 10–0325 respectively. The particle size (D) of synthesized Fe_2O_3 was 11.45–42.40 nm, TiO_2 was 4.69–7.16 nm, and $NiFe_2O_4$ was 8.53–111.98 nm. The average particle size (D_{av}) for Fe_2O_3, TiO_2, and $NiFe_2O_4$ was found to be 28.68, 5.72 and 56.65 nm respectively.

3.2. SEM analysis of nanoparticles

The SEM image of fabricated Fe_2O_3, TiO_2 and $NiFe_2O_4$ nanoparticles are represented in figure 2. The SEM image confirms the formations of nanoparticles which agrees with the result found from the XRD analysis. The figure represents that the produced Fe_2O_3 and $NiFe_2O_4$ nanoparticles are irregular in shape, whereas, TiO_2 nanoparticles is almost spherical in shape. Although some particles are agglomerated, most of the particles can be identified by the nanometer scale are termed as primary particles. Typical nanoparticles are agglomerates of several primary particles. The agglomerates are termed as secondary particles. They formed when primary particles are held together by weak surfaces forces (soft agglomerates) such as van der Waals or capillary forces or by strong chemical bonds (hard agglomerates).

3.3. EDS analysis of nanoparticles

The EDS spectrum of synthesized Fe_2O_3, TiO_2, and $NiFe_2O_4$ nanoparticles are illustrated in figure 3 and tabulated in table 2. According to figure 3(a) for Fe_2O_3 nanoparticles, the kinetic energy of the emitted electrons for iron (Fe) and oxygen (O) atom was found 6.398 keV and 0.525 keV respectively. The weight compositions of Fe and O were found to be 72.86% and 27.14% respectively, which is in good agreement with the theoretical values of Fe (69.944%) and O (30.06%) in the α-Fe_2O_3 compound. According to figure 3(b) for TiO_2 nanoparticles, the kinetic energies of the emitted electrons for titanium (Ti) and oxygen (O) atom were found 4.508 keV and 0.525 keV respectively. The weight compositions of Ti and O were found to be 56.43% and 43.57% respectively, which is in good agreement with the theoretical values of Ti (59.93%) and O (40.07%) in TiO_2 compound. According to figure 3(a) for $NiFe_2O_4$ nanoparticles, the kinetic energy of the emitted electrons for nickel (Ni), iron (Fe) and oxygen (O) atom were found 7.471 keV, 6.398 keV and 0.525 keV respectively. The weight compositions of Ni, Fe, and O were found to be 19.61%, 69.31% and 11.08% respectively, which is in

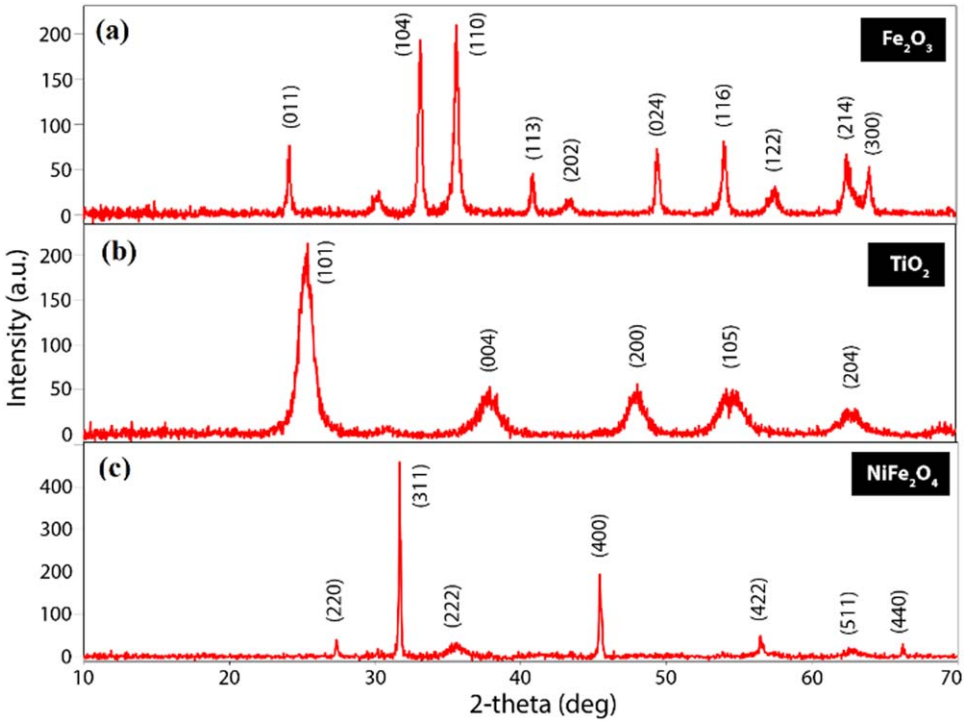

Figure 1. XRD pattern: (a) Fe_2O_3 nanoparticle synthesized by sol-gel method, (b) TiO_2 nanoparticles synthesized by sol-gel method, and (c) $NiFe_2O_4$ nanoparticles synthesized by co-precipitation method.

Table 1. Fe_2O_3, TiO_2 and $NiFe_2O_4$ nanoparticles size calculated from XRD pattern.

Nano-particle	Peak position 2θ (Deg.)	Corresponding crystal plane	FWHM (Deg.)	Particle diameter, D (nm)	Average diameter, D_{av} (nm)
	24.096	(012)	0.20	42.40	
	33.187	(104)	0.253	34.21	
	35.643	(110)	0.307	28.38	
	40.801	(113)	0.24	36.87	
	43.42	(202)	0.78	11.45	
	49.43	(024)	0.26	35.12	
Fe_2O_3	54.007	(116)	0.29	32.10	28.68
	57.45	(122)	0.81	11.68	
	62.42	(214)	0.42	23.09	
	63.98	(300)	0.31	31.55	
	25.31	(101)	1.188	7.16	
	37.973	(004)	1.806	4.86	
TiO_2	47.98	(200)	1.39	6.53	5.72
	54.55	(105)	1.99	4.69	
	62.73	(204)	1.81	5.37	
	27.36	(220)	0.13	65.66	
	31.703	(311)	0.077	111.98	
	35.36	(222)	1.02	8.53	
	45.435	(400)	0.103	87.3	
$NiFe_2O_4$	56.463	(422)	0.23	40.93	56.65
	62.93	(511)	0.85	11.44	
	66.23	(440)	0.14	70.74	

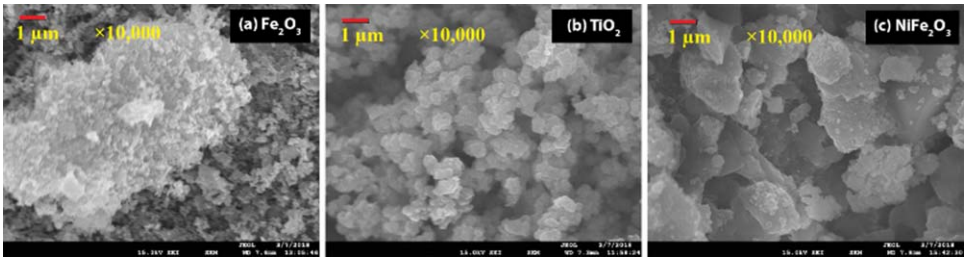

Figure 2. SEM images at 10 000 magnifications: (a) Fe_2O_3, (b) TiO_2, and (c) $NiFe_2O_4$ nanoparticles.

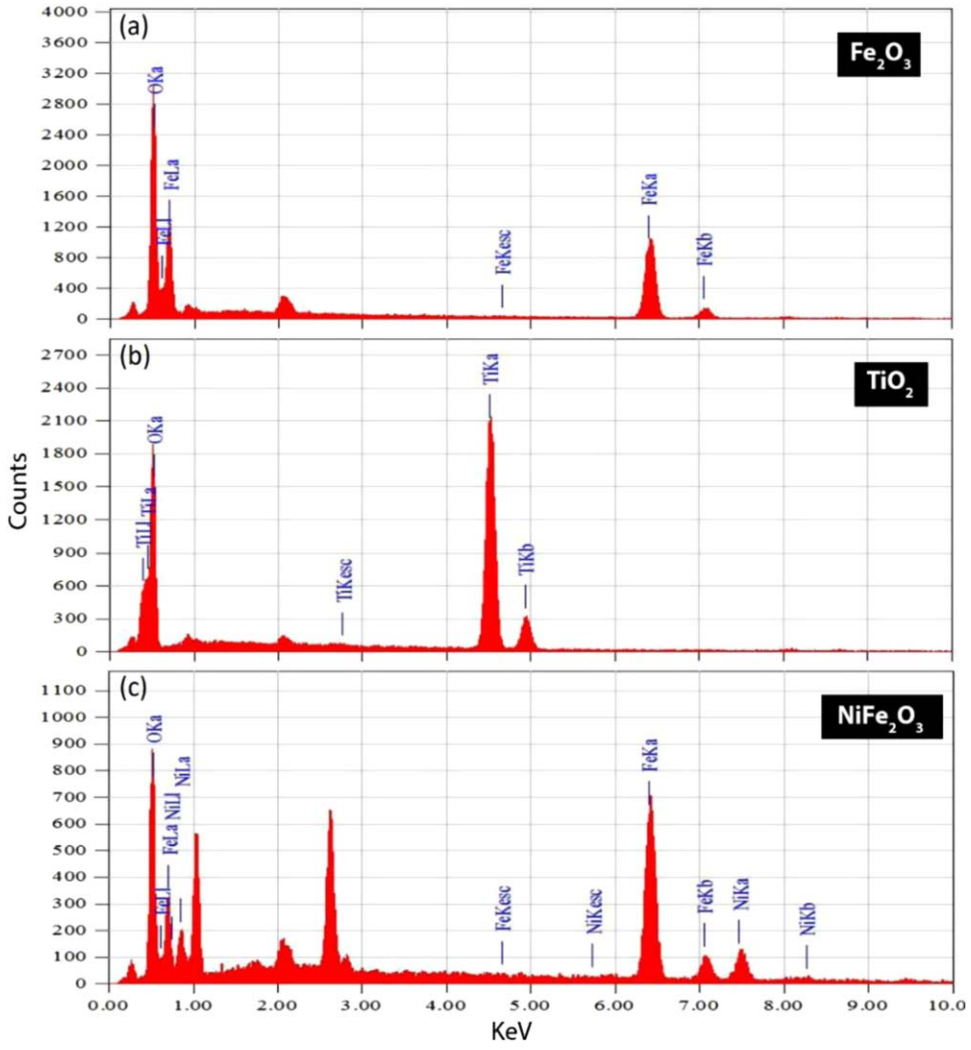

Figure 3. EDS spectra generated at 10 kV accelerating voltage: (a) Fe_2O_3, (b) TiO_2, and (c) $NiFe_2O_4$ nanoparticles.

good agreement with those of the theoretical values of Ni (25%), Fe (47.7%) and O (19.7%) in the $NiFe_2O_4$ compound. All represented data above confirms the formation of pure Fe_2O_3, TiO_2, and $NiFe_2O_4$ nanoparticles.

3.4. Thermal analysis of nanocomposites

Figure 4 represents the TGA curves of all nanocomposite samples and the results are also tabulated in table 3. According to figure 4 it is seen that this is one step decomposition process. Minor weight loss occurred between 25 to 400 °C due to evaporation of water and liberation of CO and CO_2 gases [28]. Significant weight loss occurred for HDPE between 454 to 501 °C (which is similar to the previously reported results [29]), Fe_2O_3/HDPE between 476.9 to 509.5 °C, TiO_2/HDPE between 469.6 to 507.9 °C, $NiFe_2O_4$/HDPE between 466.9 to 506.2 °C and (Fe_2O_3/TiO_2/$NiFe_2O_4$)/HDPE between 476.2 to 508.3 °C molecular interaction,

Table 2. Comparison of atomic mass percentage for Fe_2O_3, TiO_2 and $NiFe_2O_4$ nanoparticles obtained from EDS with theoretical values.

			Atomic mass percentage (%)	
Nano-particle sample	Elements	Electron ejection energy (KeV)	Calculated value	Theoretical value
Fe_2O_3	Fe	6.398	72.86	69.944
	O	0.525	27.14	30.06
TiO_2	Ti	4.508	56.43	59.93
	O	0.525	43.57	40.07
$NiFe_2O_4$	Ni	7.471	19.61	25
	Fe	6.398	69.31	47.7

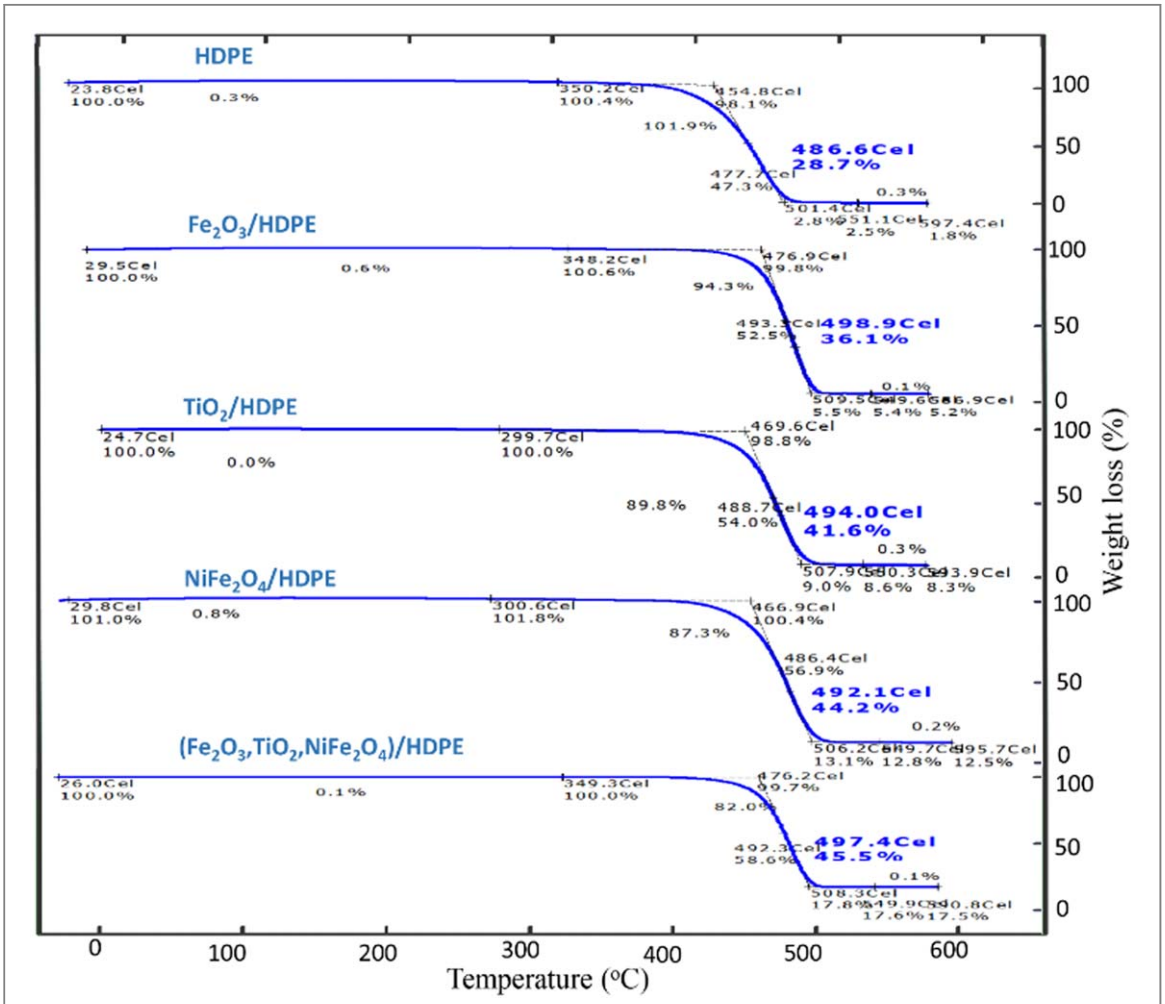

Figure 4. TGA curve for HDPE and HDPE polymer matrix nanocomposites.

Table 3. Thermal decomposition data for HDPE and HDPE nanocomposites.

Sample name	Degradation temperature (°C)	Residual (%)
HDPE	454–501	1.8
Fe_2O_3/HDPE	476.9–509.5	5.2
TiO_2/HDPE	469.6–507.9	8.3
$NiFe_2O_4$/HDPE	466.9–506.2	12.5
(Fe_2O_3/TiO_2/$NiFe_2O_4$)/HDPE	476.2–508.3	17.5

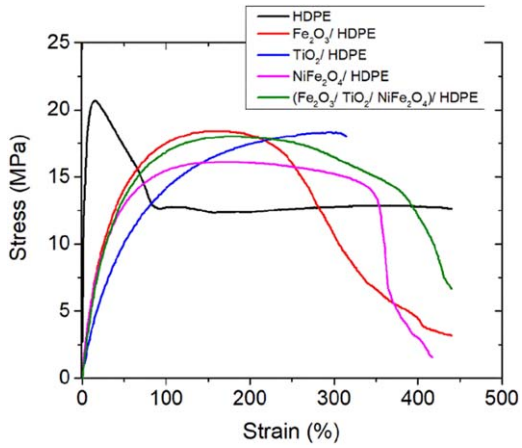

Figure 5. Stress-strain curve for HDPE and HDPE polymer matrix nanocomposites.

complex formation and dehydration of –OH groups in nanoparticles [30]. Above this temperature and up to the end the weight loss remains constant. The nano-sized particles being present in the polymer matrix reduced the motion of molecular chain of the polymer [31] by increasing molecular weight of the polymer [32]. Also, the low thermal conducting nanoparticles acted as barrier medium to hinder the diffusion of volatile products produced during the decomposition of the composites [33] resulting low thermal degradation of the polymer composite.

Above this degradation temperature ranges the weight remains constant and the residual weights found at around 594 °C are approximately 1.8, 5.2, 8.3, 12.5 and 17.5% for HDPE, Fe_2O_3/HDPE, TiO_2/HDPE, $NiFe_2O_4$/HDPE and (Fe_2O_3/TiO_2/$NiFe_2O_4$)/HDPE composites respectively. The nanocomposites left higher percentages of residues which might be assumed as the weight of the respective loaded nanoparticles and its organometallic complexes. Among the nanocomposites, $NiFe_2O_4$/HDPE as well as Fe_2O_3/TiO_2/$NiFe_2O_4$)/HDPE nanocomposites gave higher residual weights of 12.5 and 17.5% respectively at the high temperature at around 594 °C, $NiFe_2O_4$ nanoparticle more preferably interact with fragments of HDPE units forming a stable metal complex resulting higher residual weight. This phenomenon also reflected more significantly in the case of (Fe_2O_3/TiO_2/$NiFe_2O_4$)/HDPE composite giving 17.5% residual weight. Thus in presence of nanoparticles, the polymer becomes more thermally stable compared to the pure HDPE polymer.

3.5. Mechanical test of nanocomposites

3.5.1. Tensile test

The stress-strain curve (Tensile) for HDPE based nanocomposites are represented in figure 5. The curves have two regions- one is the elastic region where composites deform elastically and another is the plastic region from where plastic deformation starts. The stress of the pure HDPE reaching at maximum (above 20 MPa) falls quickly to 12.5 MPa and remains almost constant with continuous strain up to the end, whereas, all nanocomposites showed lower stress and they all fractured within 450% of their strain due to stiffening effect of nanoparticles.

The figures 6(a)–(c) show the effect of different nanoparticles addition on tensile strength, Young's modulus and fracture energy respectively in HDPE polymer matrix. According to the figure 6(a), the tensile strength of pure HDPE was found 20.084 MPa (which is similar to the previously reported results [34]) which is higher than any nanocomposite. The respective tensile strength found for the addition of Fe_2O_3, TiO_2, $NiFe_2O_4$ and (Fe_2O_3/TiO_2/$NiFe_2O_4$) nanoparticles into the polymer was 19.64, 18.18 (which is consistent with previously reported results [35]), 15.97 and 18.14 MPa which is respectively 2.21%, 9.48%, 20.46% and 9.67% lower than the HDPE polymer alone. The lowest tensile strength was found in the $NiFe_2O_4$/HDPE nanocomposite. This might be due to the bigger size of $NiFe_2O_4$ nanoparticles which restricted this nanoparticle to fill inter molecular spaces compared to other smaller nanoparticles. The mechanical properties of nanoparticles dispersed polymer composites do not always improve [36]. Nanoparticles have high surface energy with a greater tendency to agglomerate [37] and agglomerated nanoparticles are shown in SEM images. Thus, the agglomerated nanoparticles which acted as stress-concentrating centres inside the HDPE matrix are responsible for lower tensile strength in nanocomposites. Some inherent defects were produced such as voids, holes during fabrication of nanocomposites by simple melt mixing process which is another reason for the reduction of the tensile strength in fabricated composites [38]. Moreover, inorganic nanoparticles are hydrophilic so they are not compatible with the hydrophobic polymer [39] such as HDPE; therefore, the interfacial adhesion was not strong

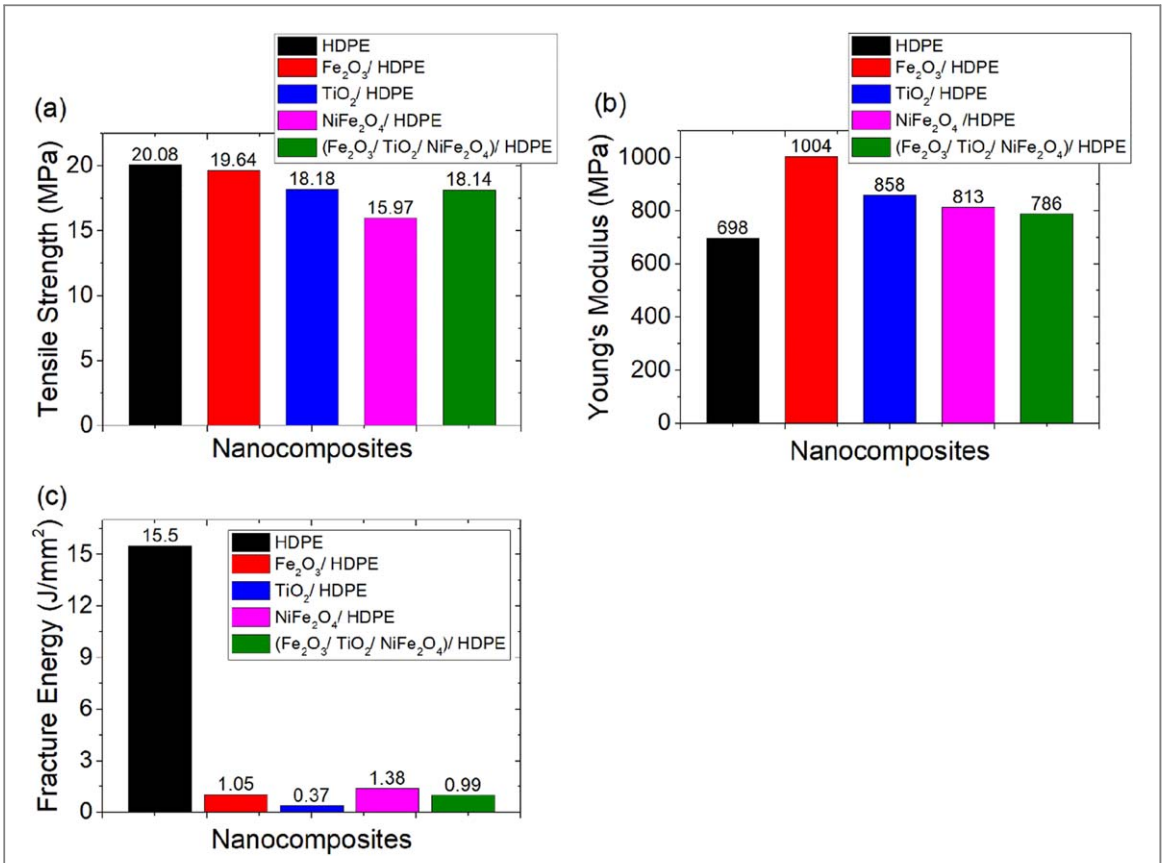

Figure 6. Effect of nanoparticles addition on (a) Tensile strength, (b) Young's modulus, and (c) Fracture energy in HDPE and HDPE polymer matrix nanocomposites.

enough to stand up to large mechanical forces resulting in lower tensile strength [40]. Due to having lower tensile strength, those composites will tear apart under lower tensile load compared to pure HDPE polymer.

According to figure 6(b), the investigated young's modulus of HDPE was found 698 (previously reported 606.3 MPa [41]) MPa, which is lower than any nanocomposite. The respective Young's modulus found for the addition of Fe_2O_3, TiO_2, $NiFe_2O_4$, and (Fe_2O_3/TiO_2/$NiFe_2O_4$) nanoparticles into the polymer matrix were 1004, 858 MPa [35], 813 and 786 MPa which is respectively 43.83%, 22.92%, 16.47%, and 12.60% higher than the HDPE polymer alone. The highest Young's modulus was found in the Fe_2O_3/HDPE nanocomposite. The presence of highly stiff nanoparticles in the polymer matrix is responsible for increasing the Young's modulus of the HDPE polymer [42]. The deformation of the HDPE polymer becomes reduced, because with nano-size the particles can easily fill the intermolecular space of the polymer as well as can resist the dislocation movement which makes the polymer much hard and brittle [37]. Consequently, the composite can bear more loads compared with pure HDPE polymer resulting in higher Young's modulus.

According to the figure 6(c), the experimental value of fracture energy for HDPE was found 15.5 J mm^{-2}, which is higher than any nanocomposite. The respective fracture energy found for the addition of Fe_2O_3, TiO_2, $NiFe_2O_4$ and (Fe_2O_3/TiO_2/$NiFe_2O_4$) nanoparticles into the polymer matrix was 1.05, 0.3, 1.38 and 0.99 J mm^{-2} which is respectively 93.22%, 97.61%, 91.41% and 93.61% lower than the HDPE polymer alone. The lowest fracture energy was found in TiO_2/HDPE nanocomposite. However, in presence of nanoparticles the matrix becomes less elastic causing less deformation resulting overall reduction of strain [37]; therefore, less energy is needed to tear the composites which reduce the total area under the stress-strain curve. Thus the fracture energy of the nanocomposites becomes lower than the pure HDPE polymer matrix. Due to having lower fracture energy a lesser amount of load will be required to fracture the composite compared to the pure HDPE polymer.

3.5.2. Microhardness test

Figure 7 shows the variation of Vicker's hardness of the fabricated nanocomposites for the addition of different nanomaterials in HDPE polymer matrix at same loading. The Vicker's hardness number of HDPE, Fe_2O_3/HDPE, TiO_2/HDPE, $NiFe_2O_4$/HDPE and (Fe_2O_3/TiO_2/$NiFe_2O_4$)/HDPE samples under 98.07 mN, 245.2 mN and 490.3 mN load were found {5.09, 5.12, 6.08, 4.41, 5.03 HV}, {5.54, 5.61, 5.91, 4.40, 5.91 HV} and {5.37, 5.42, 6.11, 4.56, 5.60 HV} respectively. It is observed that due to the addition of Fe_2O_3, TiO_2 as well as

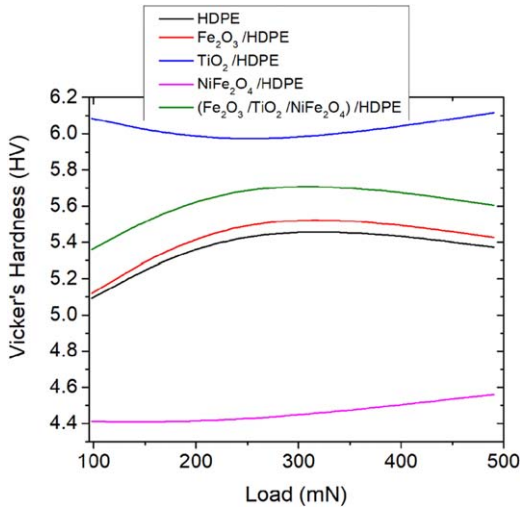

Figure 7. Effects of different nanomaterials addition on the hardness of HDPE and HDPE polymer matrix nanocomposites.

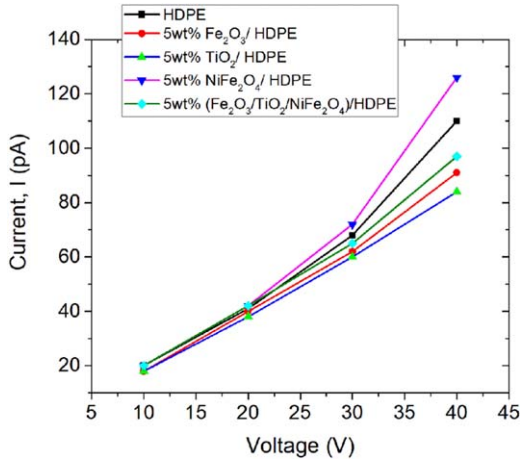

Figure 8. Effect of nanoparticles addition on I–V characteristics in HDPE and HDPE polymer matrix nanocomposites.

($Fe_2O_3/TiO_2/NiFe_2O_4$) nanomaterials in HDPE polymer matrix the hardness number was increased. In this case, the fillers act as load bearing material, thus, deformation due to indentation was reduced. In addition, well dispersion of nanoparticles and high binding affinity of the fillers with the HDPE polymer also favoured the process. Due to increasing hardness, the composite becomes more stable under penetration or scratch. In contrary, due to addition of $NiFe_2O_4$ nanoparticles the hardness value decreased. This can be attributed to the non-uniform dispersion of $NiFe_2O_4$ nanoparticles due to the bigger size compared to other nanoparticles and agglomeration of this nanoparticles into the HDPE matrix. However, several surface treatments can be done to prevent nanomaterials from agglomeration to utilize their unique characteristics in composite materials.

3.6. DC electrical studies of nanocomposites

The effect of nanoparticles addition on I–V characteristics curve and resistivity of HDPE polymer is illustrated in figures 8 and 9 respectively. According to figure 8, it is seen that DC electrical conductance of HDPE increased due to the addition of $NiFe_2O_4$ nanomaterials, whereas, the conductance decreased due to the addition of TiO_2, Fe_2O_3 and ($Fe_2O_3/TiO_2/NiFe_2O_4$) nanomaterials. Here the current increased almost linearly in response to increased voltage. The maximum current conduction was observed for the $NiFe_2O_4$/HDPE composite, whereas, the lowest conduction was observed for TiO_2/HDPE composite. Due to having lower conductance, the composite becomes more electrically insulator.

According to figure 9, the resistivity of pure HDPE polymer was found 5.79×10^{10} Ω.cm. The resistivity of Fe_2O_3/HDPE, TiO_2/HDPE and ($Fe_2O_3/TiO_2/NiFe_2O_4$)/HDPE composite were found 6.39×10^{10}, 6.62×10^{10} and 5.98×10^{10} Ω.cm respectively, all that are higher than the HDPE polymer matrix alone. In

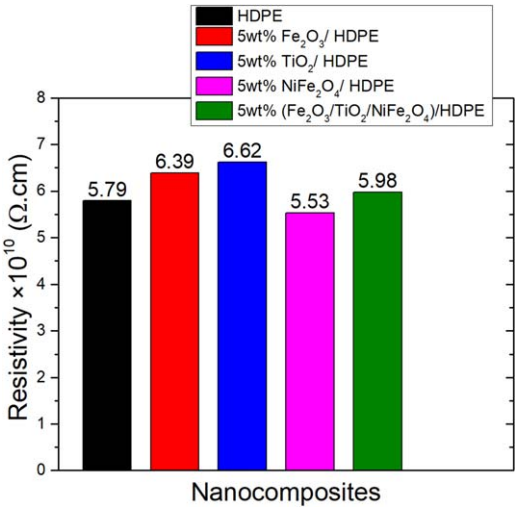

Figure 9. Effect of nanoparticles addition on resistivity in HDPE and HDPE polymer matrix nanocomposites.

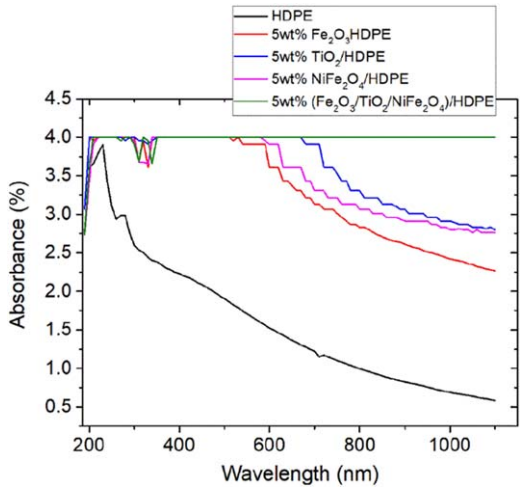

Figure 10. Variation of absorbance with wavelength for HDPE and HDPE polymer matrix nanocomposites.

contrast, the lowest resistivity was found in $NiFe_2O_4$/HDPE composite which was 5.53 $\times$ 10^{10} Ω.cm. Thus, the nanoparticles make the composites as a good candidate material where electrical insulation is needed.

The lowered conductance can be attributed to the formation of deep traps at the interface between nanoparticles and matrix material [43, 44]. These interfacial traps were produced during the mixing of nanoparticles with molten HDPE polymer by hot compression molding method [38]. At the time of current flow, the charge carriers were captured in the deep tarps and carrier mobility was reduced resulting in higher resistivity [45]. In contrast, due to percolation threshold [46], $NiFe_2O_4$ nanoparticles agglomerated to create a continuous path (percolated path) and formed a conductive pattern. Besides, the bigger size of the $NiFe_2O_4$ nanoparticles also helped to form this conductive path. Thus the tunneling effect became responsible for increasing conductance as well as decreasing resistivity in the $NiFe_2O_4$/HDPE composite.

3.7. Optical properties of nanocomposites

The Ultraviolet-Visible light absorption spectra for pure HDPE polymer and fabricated nanocomposites are presented in figure 10. It is seen that, due to the addition of Fe_2O_3, TiO_2, $NiFe_2O_4$ as well as (Fe_2O_3/TiO_2/$NiFe_2O_4$) nanoparticles in the HDPE polymer matrix, the absorption spectra between the UV–vis range was shifted to higher wavelength resulting in higher light absorption. Most significantly, linear absorption spectra in the UV–vis range was seen for the (Fe_2O_3/TiO_2/$NiFe_2O_4$)/HDPE nanocomposite, thus, the highest light absorption was found for this nanocomposite. The higher light absorption proves the higher light shielding efficiency of nanocomposites in the UV–vis range than the pure HDPE polymer.

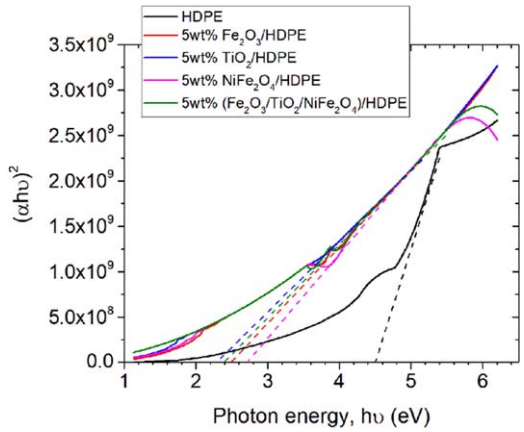

Figure 11. Optical band gap of HDPE and HDPE polymer matrix nanocomposites.

Table 4. Optical band gap of HDPE and nanocomposites.

Sample name	Optical band gap energy (eV)	Decrease (%)
HDPE	4.5	—
Fe_2O_3/HDPE	2.5	44.44
TiO_2/HDPE	2.3	48.88
$NiFe_2O_4$/HDPE	2.7	40
(Fe_2O_3/TiO_2/$NiFe_2O_4$)/HDPE	2.4	46.66

The variation in optical band gap energy of fabricated nanocomposites is illustrated in figure 11 as well as tabulated in table 4. According to the figure 11 it is clear that the addition of nanoparticles is responsible for lowering the optical bandgap energy in composites. The direct optical band gap energy of pure HDPE polymer was found 4.5 eV. Due to the incorporation of Fe_2O_3, TiO_2, $NiFe_2O_4$ and (Fe_2O_3/TiO_2/$NiFe_2O_4$) nanoparticles the optical band gap was found 2.5, 2.3, 2.7 and 2.4 eV respectively, which is 44.44, 48.88, 40 and 46.66% lower than the pure HDPE.

The transparency of nanocomposites depends upon the size and spatial distribution of nanoparticles in the polymer matrix. The improved light absorbance is found in nanocomposites due to the successful dispersion of nanoparticles into the polymer matrix where the particles restrict the light transmission by absorbing, blocking or scattering the incident light [47]. Additionally, the opacity of nanocomposites can also be attributed to the formation of a three-dimensional network of nanoparticles within the polymer matrix; in practice, it hinders the light transmission through the material [37]. Increase in light absorption is responsible for shifting the absorption spectra to a higher wavelength, which suggests a reduction in the optical band gap energy [48]. Also, the agglomeration of nanoparticles formed clusters inside the matrix which helps to increase the nanoparticles size is another important factor for lowering band gap energy [49]. Therefore, it can be concluded that the agglomeration of nanoparticles inside matrix and light scattering at interface between nanoparticles and matrix is responsible for lowering the optical band gap of pure HDPE polymer [50].

4. Summary

In this study, 5 wt% synthesized nanoparticles dispersed high density polyethylene (HDPE) based nanocomposites were fabricated by hot compression molding method to evaluate their mechanical, optical and electrical properties. Both Fe_2O_3 and TiO_2 nanoparticles were synthesized by sol-gel method as well as $NiFe_2O_4$ nanoparticles were synthesized by co-precipitation method. The XRD, SEM and EDS data confirmed the formation of hematite (α-Fe_2O_3), anatase (TiO_2) and $NiFe_2O_4$ nanoparticles with the average size of 28.68, 5.72 and 56.64 nm respectively. Higher young's modulus, whereas, lower tensile strength as well as lower fracture energy was found in all nanocomposites. The highest Young's modulus, lowest tensile strength, and lowest fracture energy were found in Fe_2O_3/HDPE, $NiFe_2O_4$/HDPE and TiO_2/HDPE nanocomposites respectively. Hardness was increased in all composites except for $NiFe_2O_4$/HDPE composite. Higher electrical conductance

as well as lower resistivity was found in $NiFe_2O_4$/HDPE composite and opposite behavior was seen in the rest of the composites. The higher light absorbance in the UV–vis range and lower optical bandgap energy were found in all nanocomposites. The highest absorbance and lowest bandgap energy were found in (Fe_2O_3/TiO_2/$NiFe_2O_4$)/HDPE and TiO_2/HDPE nanocomposites respectively. To the end, these newly fabricated composites can be useful for biomedical applications, electromagnetic wave and UV shielding, super capacitor as well as other industrial purposes.

Acknowledgments

This research work has been done with the financial support of University Grants Commission (UGC) of Bangladesh through the Faculty of Engineering, University of Rajshahi. The researchers acknowledge the supports of Bangladesh Council of Scientific and Industrial Research (BCSIR) and Bangladesh Atomic Energy Commission (BAEC) for the permission of using the laboratory facilities.

Conflicts of interest

The authors declare that they have no competing interests.

ORCID iDs

M Khalid Hossain https://orcid.org/0000-0003-4595-6367

References

[1] Sanchez C, Julián B, Belleville P and Popall M 2005 Applications of hybrid organic–inorganic nanocomposites *J. Mater. Chem.* **15** 3559
[2] Sui G, Zhong W H, Ren X, Wang X Q and Yang X P 2009 Structure, mechanical properties and friction behavior of UHMWPE/HDPE/carbon nanofibers *Mater. Chem. Phys.* **115** 404–12
[3] Gusev A A and Lusti H R 2001 Rational design of nanocomposites for barrier applications *Adv. Mater.* **13** 1641–3
[4] Balakrishnan H, Husin M R, Wahit M U and Abdul Kadir M R 2014 Preparation and characterization of organically modified montmorillonite-filled high density polyethylene/hydroxyapatite nanocomposites for biomedical applications *Polym. Plast. Technol. Eng.* **53** 790–800
[5] Willie B M, Bloebaum R D, Ashrafi S, Dearden C, Steffensen T and Hofmann A A 2006 Oxidative degradation in highly cross-linked and conventional polyethylene after 2 years of real-time shelf aging⋆ *Biomaterials* **27** 2275–84
[6] Tadic M, Panjan M, Damnjanovic V and Milosevic I 2014 Magnetic properties of hematite (α-Fe_2O_3) nanoparticles prepared by hydrothermal synthesis method *Appl. Surf. Sci.* **320** 183–7
[7] Stanciu L, Won Y-H, Ganesana M and Andreescu S 2009 Magnetic Particle-Based Hybrid Platforms for Bioanalytical Sensors *Sensors* **9** 2976–99
[8] Vijayanand H V, Arunkumar L, Gurubasawaraj P M, Sharma P M V, Basavaraja S, Saleem A, Venkataraman A, Ghanwat A and Maldar N N 2007 Synthesis and characterization of polyimide-γ-Fe_2O_3 nanocomposites *J. Appl. Polym. Sci.* **103** 834–40
[9] Chen J-H, Dai C-A, Chen H-J, Chien P-C and Chiu W-Y 2007 Synthesis of nano-sized TiO_2/poly(AA-co-MMA) composites by heterocoagulation and blending with PET *J. Colloid Interface Sci.* **308** 81–92
[10] Kandulna R, Choudhary R B and Singh R 2018 TiO2 reinforced PMMA-TiO2 nanocomposite for its application in organic light emitting diode (OLED) as electron transport layer material *AIP Conference Proceedings* **1942** 110057
[11] Bodaghi H, Mostofi Y, Oromiehie A, Ghanbarzadeh B and Hagh Z G 2015 Synthesis of clay-TiO_2 nanocomposite thin films with barrier and photocatalytic properties for food packaging application *J. Appl. Polym. Sci.* **132** 41764
[12] Pozar D M and Kaufman B 1987 Increasing the bandwidth of a microstrip antenna by proximity coupling *Electron. Lett* **23** 368
[13] Balaji S, Kalai Selvan R, John Berchmans L, Angappan S, Subramanian K and Augustin C O 2005 Combustion synthesis and characterization of Sn^{4+} substituted nanocrystalline $NiFe_2O_4$ *Mater. Sci. Eng.* B **119** 119–24
[14] Singh J, Srivastava M, Kalita P and Malhotra B D 2012 A novel ternary $NiFe_2O_4$/CuO/FeO-chitosan nanocomposite as a cholesterol biosensor *Process Biochem.* **47** 2189–98
[15] Sunny V, Kurian P, Mohanan P, Joy P A and Anantharaman M R 2010 A flexible microwave absorber based on nickel ferrite nanocomposite *J. Alloys Compd.* **489** 297–303
[16] Balakrishnan H, Husin M R, Wahit M U and Abdul Kadir M R 2013 Maleated high density polyethylene compatibilized high density polyethylene/hydroxyapatite composites for biomedical applications: properties and characterization *Polym. Plast. Technol. Eng.* **52** 774–82
[17] Chrissafis K, Paraskevopoulos K M, Pavlidou E and Bikiaris D 2009 Thermal degradation mechanism of HDPE nanocomposites containing fumed silica nanoparticles *Thermochim. Acta* **485** 65–71
[18] Lee Y H, Park C B, Sain M, Kontopoulou M and Zheng W 2007 Effects of clay dispersion and content on the rheological, mechanical properties, and flame retardance of HDPE/clay nanocomposites *J. Appl. Polym. Sci.* **105** 1993–9
[19] Trujillo M, Arnal M L, Müller A J, Laredo E, Bredeau S, Bonduel D and Dubois P 2007 Thermal and morphological characterization of nanocomposites prepared by *in-situ* polymerization of high-density polyethylene on carbon nanotubes *Macromolecules* **40** 6268–76
[20] Jung J, Kim J, Uhm Y R, Jeon J-K, Lee S, Lee H M and Rhee C K 2010 Preparations and thermal properties of micro- and nano-BN dispersed HDPE composites *Thermochim. Acta* **499** 8–14
[21] Minkova L, Peneva Y, Tashev E, Filippi S, Pracella M and Magagnini P 2009 Thermal properties and microhardness of HDPE/clay nanocomposites compatibilized by different functionalized polyethylenes *Polym. Test.* **28** 528–33

[22] Hoque M A, Ahmed M R, Rahman G T, Rahman M T, Islam M A, Khan M A and Hossain M K 2018 Fabrication and comparative study of magnetic Fe and α-Fe_2O_3 nanoparticles dispersed hybrid polymer (PVA + Chitosan) novel nanocomposite film *Results Phys.* **10** 434–43
[23] Kamil F, Hubiter K A, Abed T K and Al-Amiery A A 2016 Synthesis of aluminum and titanium oxides nanoparticles via sol-gel method: optimization for the minimum size *J. Nanosci. Tech.* **2** (1) 37–39
[24] Maaz K, Karim S, Mumtaz A, Hasanain S K, Liu J and Duan J L 2009 Synthesis and magnetic characterization of nickel ferrite nanoparticles prepared by co-precipitation route *J. Magn. Magn. Mater.* **321** 1838–42
[25] Rahman M T, Asadul Hoque M, Rahman G T, Gafur M A, Khan R A and Hossain M K 2019 Study on the mechanical, electrical and optical properties of metal-oxide nanoparticles dispersed unsaturated polyester resin nanocomposites *Results Phys.* **13** 102264
[26] Rahman M T, Hoque M A, Rahman G T, Azmi M M, Gafur M A, Khan R A and Hossain M K 2019 Fe_2O_3 nanoparticles dispersed unsaturated polyester resin based nanocomposites: effect of gamma radiation on mechanical properties *Radiat. Eff. Defects Solids* 1–14
[27] Tauc J 1968 Optical properties and electronic structure of amorphous Ge and Si *Mater. Res. Bull.* **3** 37–46
[28] Purohit V and Orzel R A 1988 Polypropylene: a literature review of the thermal decomposition products and toxicity *J. Am. Coll. Toxicol.* **7** 221–42
[29] Awad A H, Aly Abd El-Wahab A, El-Gamsy R and Abdel-latif M H 2019 A study of some thermal and mechanical properties of HDPE blend with marble and granite dust *Ain Shams Eng. J.*. (https://doi.org/10.1016/j.asej.2018.08.005)
[30] Guo Z, Lei K, Li Y, Ng H W, Prikhodko S and Hahn H T 2008 Fabrication and characterization of iron oxide nanoparticles reinforced vinyl-ester resin nanocomposites *Compos. Sci. Technol.* **68** 1513–20
[31] Corcione C and Frigione M 2012 Characterization of nanocomposites by thermal analysis *Materials (Basel)* **5** 2960–80
[32] Abdul Kaleel S H, Bahuleyan B K, Masihullah J and Al-Harthi M 2011 Thermal and mechanical properties of polyethylene/doped-TiO_2 nanocomposites synthesized using *in situ* polymerization *J. Nanomater.* **2011** 1–6
[33] Leszczyńska A, Njuguna J, Pielichowski K and Banerjee J R 2007 Polymer/montmorillonite nanocomposites with improved thermal properties *Thermochim. Acta* **453** 75–96
[34] Huang R, Xu X, Lee S, Zhang Y, Kim B-J and Wu Q 2013 High density polyethylene composites reinforced with hybrid inorganic fillers: morphology, mechanical and thermal expansion performance *Materials (Basel)* **6** 4122–38
[35] Mozumder M S, Mourad A-H I, Mairpady A, Pervez H and Haque M E 2018 Effect of TiO_2 nanofiller concentration on the mechanical, thermal and biological properties of HDPE/TiO_2 nanocomposites *J. Mater. Eng. Perform.* **27** 2166–81
[36] Lee H-T and Lin L-H 2006 Waterborne polyurethane/clay nanocomposites: novel effects of the clay and its interlayer ions on the morphology and physical and electrical properties *Macromolecules* **39** 6133–41
[37] Jeon I-Y and Baek J-B 2010 Nanocomposites derived from polymers and inorganic nanoparticles *Materials (Basel)* **3** 3654–74
[38] Zhang X and Simon L C 2005 *In situ* polymerization of hybrid polyethylene-alumina nanocomposites *Macromol. Mater. Eng.* **290** 573–83
[39] Islam M S, Masoodi R and Rostami H 2013 The effect of nanoparticles percentage on mechanical behavior of silica-epoxy nanocomposites *J. Nanosci.* **2013** 1–10
[40] Chae D W and Kim B C 2005 Characterization on polystyrene/zinc oxide nanocomposites prepared from solution mixing *Polym. Adv. Technol.* **16** 846–50
[41] Tanniru M, Yuan Q and Misra R D 2006 On significant retention of impact strength in clay–reinforced high-density polyethylene (HDPE) nanocomposites *Polymer (Guildf)* **47** 2133–46
[42] Kanagaraj S, Varanda F R, Zhil'tsova T V, Oliveira M S A and Simões J A O 2007 Mechanical properties of high density polyethylene/carbon nanotube composites *Compos. Sci. Technol.* **67** 3071–7
[43] Wang Y, Xiao K, Wang C, Yang L and Wang F 2016 Effect of nanoparticle surface modification and filling concentration on space charge characteristics in TiO_2/XLPE nanocomposites *J. Nanomater.* **2016** 1–10
[44] Wu K, Chen X, Liu X, Wang X, Cheng Y and Dissado L A 2011 Study of the space charge behavior in polyethylene nano-composites under temperature gradient *Proc. of 2011 Int. Symp. on Electrical Insulating Materials (IEEE)* pp 84–7
[45] Su S-J and Kuramoto N 2000 Processable polyaniline–titanium dioxide nanocomposites: effect of titanium dioxide on the conductivity *Synth. Met.* **114** 147–53
[46] Hong J I, Winberg P, Schadler L S and Siegel R W 2005 Dielectric properties of zinc oxide/low density polyethylene nanocomposites *Mater. Lett.* **59** 473–6
[47] Ederth J, Johnsson P, Niklasson G A, Hoel A, Hultåker A, Heszler P, Granqvist C G, van Doorn A R, Jongerius M J and Burgard D 2003 Electrical and optical properties of thin films consisting of tin-doped indium oxide nanoparticles *Phys. Rev.* B **68** 155410
[48] Madani M 2011 Structure, optical and thermal decomposition characters of LDPE graft copolymers synthesized by gamma irradiation *Curr. Appl Phys.* **11** 70–6
[49] Abdullah O G, Aziz S B, Omer K M and Salih Y M 2015 Reducing the optical band gap of polyvinyl alcohol (PVA) based nanocomposite *J. Mater. Sci., Mater. Electron.* **26** 5303–9
[50] Bouzidi A, Omri K, Jilani W, Guermazi H and Yahia I S 2018 Influence of TiO_2 incorporation on the microstructure, optical, and dielectric properties of TiO_2/epoxy composites *J. Inorg. Organomet. Polym. Mater.* **28** 1114–26